Odd q-state clock spin-glass models in three dimensions, asymmetric phase diagrams, and multiple algebraically ordered phases

Odd q-state clock spin-glass models in three dimensions, asymmetric phase diagrams, and multiple algebraically ordered phases

Efe Ilker[1] and A. Nihat Berker[1,2]

[1]*Faculty of Engineering and Natural Sciences, Sabancı University, Tuzla 34956, Istanbul, Turkey*

[2]*Department of Physics, Massachusetts Institute of Technology, Cambridge, Massachusetts 02139, USA*

(Received 17 July 2014; published 4 December 2014)

Distinctive orderings and phase diagram structures are found, from renormalization-group theory, for odd q-state clock spin-glass models in $d = 3$ dimensions. These models exhibit asymmetric phase diagrams, as is also the case for quantum Heisenberg spin-glass models. No finite-temperature spin-glass phase occurs. For all odd $q \geqslant 5$, algebraically ordered antiferromagnetic phases occur. One such phase is dominant and occurs for all $q \geqslant 5$. Other such phases occupy small low-temperature portions of the phase diagrams and occur for $5 \leqslant q \leqslant 15$. All algebraically ordered phases have the same structure, determined by an attractive finite-temperature sink fixed point where a dominant and a subdominant pair states have the only nonzero Boltzmann weights. The phase transition critical exponents quickly saturate to the high q value.

DOI: 10.1103/PhysRevE.90.062112 PACS number(s): 64.60.De, 75.10.Nr, 05.10.Cc, 75.50.Lk

I. INTRODUCTION

Spin-glass problems [1] continue to fascinate with new orderings and phase diagrams under frustration [2] and ground-state entropy [3,4]. The extension of these models from the extensively studied Ising spin models to less simple spins offer the possibility of completely new orderings and phase diagrams. We find that odd q-state clock models are such cases. Spins in odd q-state clock models cannot be exactly antialigned with each other. Furthermore, for a given spin, its interacting neighbor has two states that give the maximally misaligned pair configuration. This fact immediately injects ground-state entropy in the presence of antiferromagnetic interactions, even without the frozen randomness of interactions of the spin-glass system.

We have calculated, from renormalization-group theory, the phase diagrams of arbitrary odd q-state clock spin-glass models in $d = 3$ dimensions. We find that these models have asymmetric phase diagrams, as is also the case for quantum Heisenberg spin-glass models [5]. They exhibit no finite-temperature spin-glass phase. For all odd $q \geqslant 5$, algebraically ordered antiferromagnetic phases occur. One such phase is dominant and occurs for all $q \geqslant 5$. Other such phases occupy a small low-temperature portion of the phase diagram and occur for $5 \leqslant q \leqslant 15$. All algebraically ordered phases have the same structure, determined by an attractive finite-temperature sink fixed point where a dominant and a subdominant pair states have the only nonzero Boltzmann weights. The phase transition critical exponents come from distinct critical fixed points, but quickly saturate to the high q value. Thus, a rich phase transition structure is seen for odd q-state spin-glass models on a $d = 3$ hierarchical lattice.

II. THE ODD q-STATE CLOCK SPIN-GLASS MODEL AND THE RENORMALIZATION-GROUP METHOD

The q-state clock models are composed of unit spins that are confined to a plane and that can only point along q angularly equidistant directions. Accordingly, the q-state clock spin-glass model is defined by the Hamiltonian

$$-\beta\mathcal{H} = \sum_{\langle ij\rangle} J_{ij}\vec{s}_i \cdot \vec{s}_j = \sum_{\langle ij\rangle} J_{ij}\cos(\theta_i - \theta_j), \tag{1}$$

where $\beta = 1/k_BT$, at site i the spin angle θ_i takes on the values $(2\pi/q)\sigma_i$ with $\sigma_i = 0,1,2,\ldots,q-1$, and $\langle ij\rangle$ denotes that the sum runs over all nearest-neighbor pairs of sites. The bond strengths J_{ij} are $+J > 0$ (ferromagnetic) with probability $1-p$ and $-J$ (antiferromagnetic) with probability p. This model becomes the Ising model for $q = 2$ and the XY model for $q \to \infty$.

The q-state clock spin-glass model, in $d = 3$ dimensions, is readily solved by a renormalization-group method that is approximate on the cubic lattice [6,7] and simultaneously exact on the hierarchical lattice [8–12]. Hierarchical lattices have been used to study a variety of spin-glass and other statistical mechanics problems [13–42]. Under rescaling, for $q > 4$, the form of the interaction as given in the rightmost side of Eq. (1) is not conserved and one must therefore express the Hamiltonian more generally, as

$$-\beta\mathcal{H} = \sum_{\langle ij\rangle} V(\theta_i - \theta_j)\,. \tag{2}$$

The energy $V(\theta_i - \theta_j)$ depends on the absolute value of the angle difference, $|(\theta_i - \theta_j)|$. Thus, the renormalization-group flows are the flows of $q/2$ interaction constants for even q and the flows of $(q-1)/2$ interaction constants for odd q. With no loss of generality, the maximum value of $V(\theta_i - \theta_j)$ is set to zero.

The renormalization-group transformation, for spatial dimensions $d = 3$ and length rescaling factor $b = 3$ (necessary for treating the ferromagnetic and antiferromagnetic correlations on equal footing), is achieved by a sequence of bond moving

$$V_{bm}(\theta_1 - \theta_2) + G_{12} = \sum_{n=1}^{b^{d-1}} V_n(\theta_1 - \theta_2) \tag{3}$$

and decimation

$$e^{V_{\rm dec}(\theta_1-\theta_4)+G_{14}} = \sum_{\theta_2,\theta_3} e^{V_1(\theta_1-\theta_2)+V_2(\theta_2-\theta_3)+V_3(\theta_3-\theta_4)}, \qquad (4)$$

where the constants G_{ij} are fixed by the requirement that the maximum value of $V(\theta_i - \theta_j)$ is zero.

The starting bimodal quenched probability distribution of the interactions, characterized by p and described above, is also not conserved under rescaling. The renormalized quenched probability distribution of the interactions is obtained by the convolution [43]

$$P'(V'(\theta_{i'j'})) = \int \left[\prod_{ij}^{i'j'} dV(\theta_{ij})P(V(\theta_{ij}))\right] \delta(V'(\theta_{i'j'}) - R(\{V(\theta_{ij})\})), \qquad (5)$$

where $R(\{V(\theta_{ij})\})$ represents the bond moving and decimation given in Eqs. (3) and (4). For numerical practicality, the bond moving and decimation of Eqs. (3) and (4) are achieved by a sequence of pairwise combination of interactions, as shown in Fig. 1(c), each pairwise combination leading to an intermediate probability distribution resulting from a pairwise convolution as in Eq. (5). We effect this procedure numerically, by generating 5000 interactions that embody the quenched probability distribution resulting from each pairwise combination. Due to the large number of phase diagrams (Figs. 2 and 3), a single realization of quenched randomness is used. Each of the generated 5000 interactions is determined by $(q-1)/2$ interaction constants. At each pairwise convolution as in Eq. (5), 5000 randomly chosen pairs are matched by Eq. (3) or (4), and a new set of 5000 is produced.

The different thermodynamic phases of the model are identified by the different asymptotic renormalization-group flows of the quenched probability distributions. For all renormalization-group flows, inside the phases and on the phase boundaries, Eq. (5) is iterated until asymptotic behavior is reached. Thus, we are able to calculate phase diagrams for any number of clock states q. Similar previous studies, on other spin-glass systems, are in Refs. [13–22].

In a previous study [21], using the above method, we have considered even values of q. In this study, we consider odd values of q and calculate the phase diagrams, which are not symmetric around $p = 0.5$. For q odd, the system does not have sublattice spin-reversal ($\theta_i \to \theta_i + \pi$) symmetry, which leads to the asymmetric phase diagrams. We obtain qualitatively new features in the phase diagrams for odd q. These features do not occur for even q.

III. CALCULATED PHASE DIAGRAMS FOR ODD q-STATE CLOCK SPIN GLASSES IN $d = 3$

Our calculated phase diagrams for the odd $q = 3,5,7,9,11,13,15,17,21,361$-state clock spin-glass models are shown in Fig. 2. The lower-temperature details of the phase diagrams are given in Fig. 3. All phase boundaries are second order.

The phase diagrams of the odd q-state clock spin-glass models are quite different from the even q phase

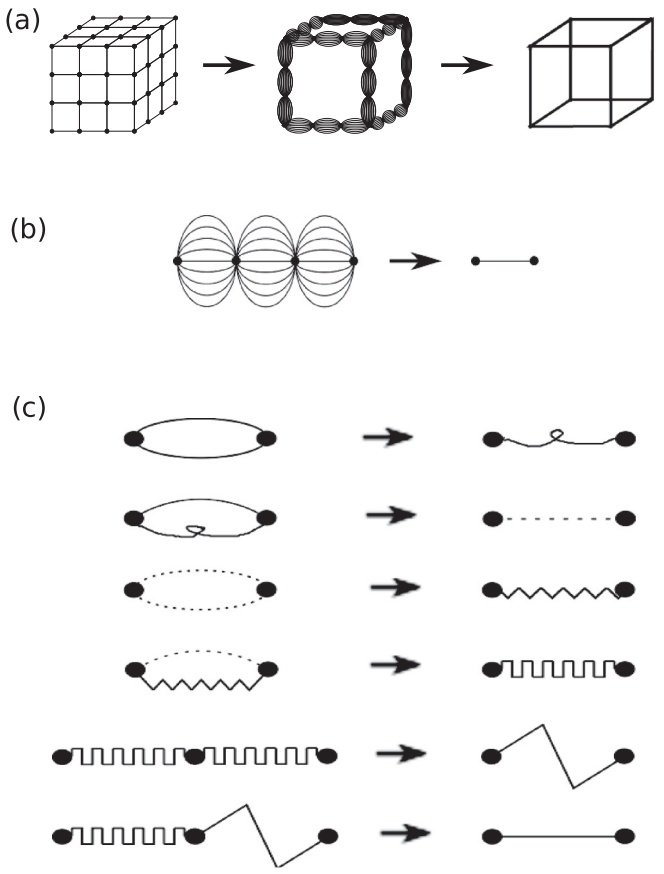

FIG. 1. (a) Migdal-Kadanoff approximate renormalization-group transformation for the $d = 3$ cubic lattice with the length-rescaling factor of $b = 3$. Bond moving is followed by decimation. (b) Exact renormalization-group transformation for the equivalent $d = 3$ hierarchical lattice with the length-rescaling factor of $b = 3$. (c) Pairwise applications of the quenched probability convolution of Eq. (5), leading to the exact transformation in (b).

diagrams [21]: The odd q phase diagrams do not have ferromagnetic-antiferromagnetic symmetry, i.e., they are not left-right symmetric with respect to the $p = 0.5$ line. The odd q phase diagrams do not have a spin-glass phase, which is consistent with previous results [13,21] that the XY model, corresponding to the $q \to \infty$ limit of the q-state clock models, does not have a spin-glass phase on $d = 3$ hierarchical lattices. The odd q phase diagrams show a multiplicity of algebraically ordered phases (and one conventionally ordered phase) on the antiferromagnetic side. All points in an algebraically ordered phase flow, under renormalization group, to a single stable fixed point (sink) that occurs at nonzero, noninfinite temperature. Convergence to this stable critical fixed occurs, to six significant figures, within five renormalization-group transformations. Further convergence is obtained for more renormalization-group transformations. As seen in Fig. 4, at each renormalization-group transformation, the quenched probability distribution of interactions changes from the initial $(1-p)$ and p double-δ function, to eventually reach the critical sink described below. Because of this flow structure, the correlation length is infinite and the correlation function decays as an inverse power of distance (as opposed to exponentially)

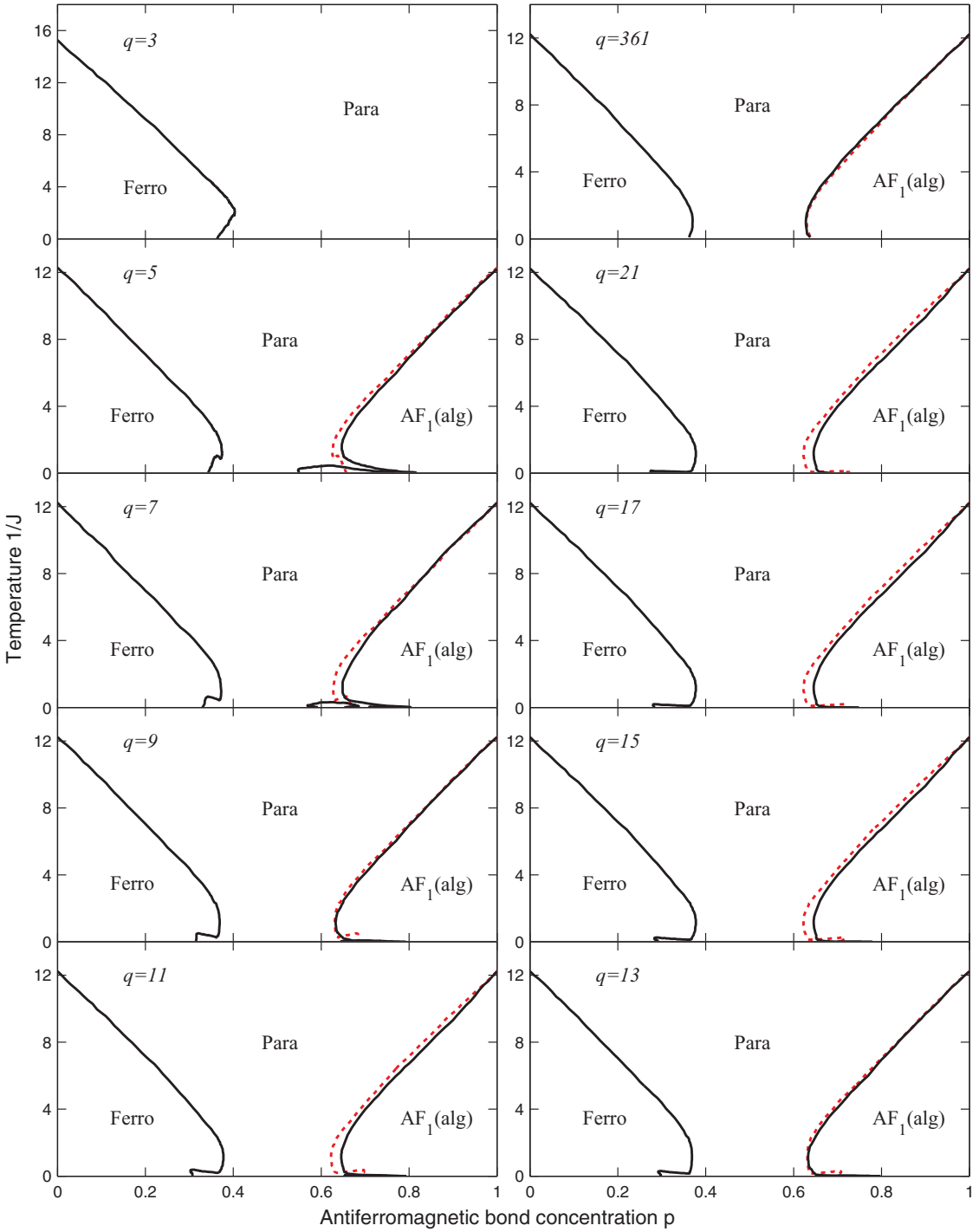

FIG. 2. (Color online) Calculated phase diagrams of the odd q-state clock spin-glass models on the hierarchical lattice with $d = 3$ dimensions. These phase diagrams do not have ferromagnetic-antiferromagnetic symmetry, i.e., they are not left-right symmetric with respect to the $p = 0.5$ line. The phase diagrams do not have a spin-glass phase, but show a multiplicity of algebraically ordered phases on the antiferromagnetic side. The phase diagrams show true reentrance (disordered-ordered-disordered) as temperature is lowered at fixed antiferromagnetic bond concentration p, on both the ferromagnetic and antiferromagnetic sides of the phase diagram. The phase diagrams also show lateral, true double reentrance (ferromagnetic-disordered-ferromagnetic-disordered) as the antiferromagnetic bond concentration p is increased at fixed temperature, only on the ferromagnetic side. No antiferromagnetic ordering occurs for the lowest model, $q = 3$. Algebraically ordered antiferromagnetic phases occur for all higher $q \geqslant 5$ models. In these cases, the phase boundary between the dominant antiferromagnetic algebraically ordered phase and the disordered phase is slightly asymmetric with the phase boundary between the ferromagnetic and disordered phases. To make this slight asymmetry evident, the latter boundary is also shown (dashed) reflected about the $p = 0.5$ line. The lower temperature details of these phase diagrams are shown in Fig. 3.

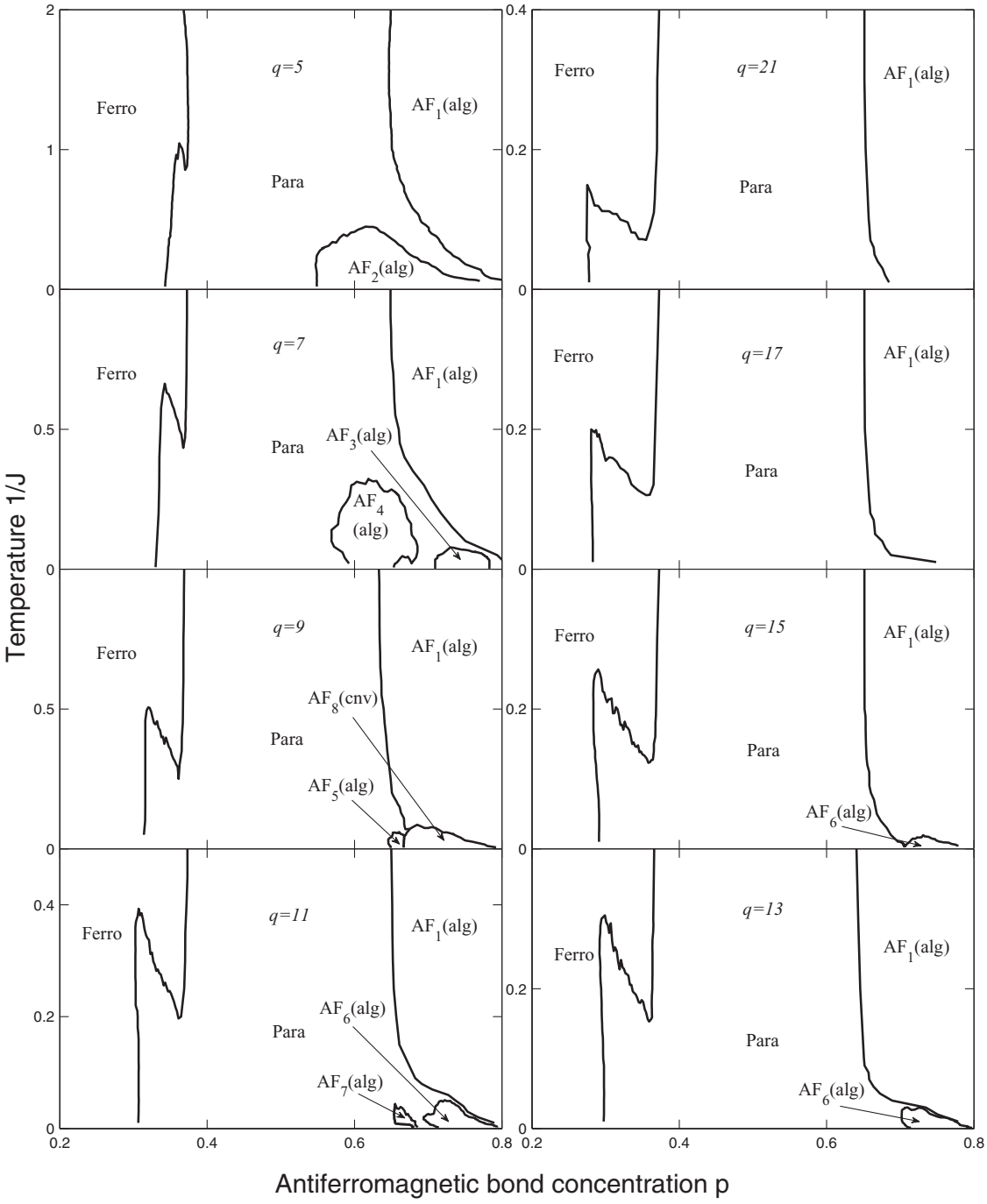

FIG. 3. Lower-temperature details of the phase diagrams shown in Fig. 2.

at all points in such an algebraically ordered phase. Such algebraically ordered phases were previously seen by Berker and Kadanoff [3,4] for antiferromagnetic Potts models and have since been extensively studied [44–52]. The correlation function decay critical exponent has the same value for all points in such a phase, since the renormalization-group flows are to single fixed point, in contrast to the continuously varying critical exponents in the algebraically ordered phase of the $d = 2$ XY model, where the flows are to a fixed line [53–55].

The phase diagrams show true reentrance [13] (disordered-ordered-disordered) as temperature is lowered at fixed antiferromagnetic bond concentration p, on both the ferromagnetic and antiferromagnetic sides of the phase diagram. The phase diagrams also show lateral, true double reentrance (ferromagnetic-disordered-ferromagnetic-disordered) as the antiferromagnetic bond concentration p is increased at fixed temperature, only on the ferromagnetic side. Multiple reentrances have previously been seen in liquid crystal systems [56–59].

No antiferromagnetic ordering occurs for the lowest model, $q = 3$. Algebraically ordered antiferromagnetic phases occur for all higher $q \geqslant 5$ models. In these cases, the phase boundary between the dominant antiferromagnetic algebraically ordered phase and the disordered phase is slightly asymmetric with

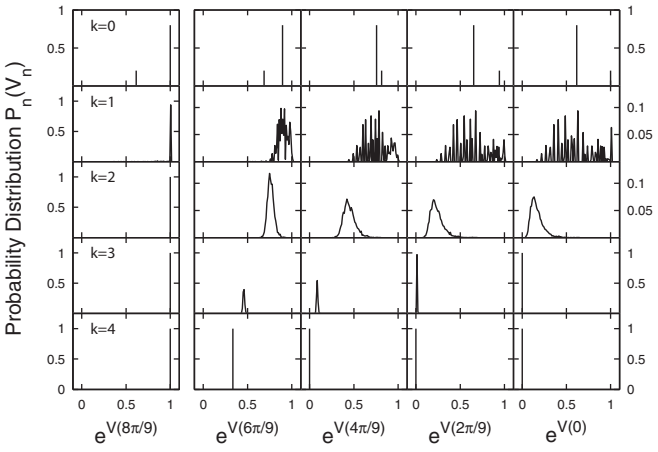

FIG. 4. Evolution of the quenched probability distribution under successive renormalization-group transformations. The case of $q = 9$, starting with the initial condition temperature $1/J = 4$ and antiferromagnetic bond concentration $p = 0.8$ is shown here. For $q = 9$, the generalized interaction potential unavoidably generated by the renormalization-group transformation is determined by four interaction constants (see Table I). The renormalization-group transformation gives the evolution, under scale change, of the correlated quenched probability distribution $P(V_0, V_1, V_2, V_3, V_4)$. Shown in this figure are the projections $P_0(V_0) = \int dV_1 dV_2 dV_3 dV_4 P(V_0, V_1, V_2, V_3, V_4)$ and similarly for $P_1(V_1), P_2(V_2), P_3(V_3)$, and $P_4(V_4)$. Each row corresponds to another renormalization-group step k, as marked on the figure. It is seen here that in four renormalization-group transformations, the renormalized system essentially reaches the critical phase sink described in Sec. IV: The most misaligned pair state is dominant with Boltzmann weight $e^{V(8\pi/9)} = 1$ and the next-most misaligned pair state is also present but less dominant with $e^{V(6\pi/9)} = 1/3$. The other two less misaligned pair states and the aligned pair state have zero Boltzmann weight at the sink.

the phase boundary between the ferromagnetic phase and the disordered phase. To make this slight asymmetry evident, the latter boundary is also shown (dashed) in Fig. 2 reflected about the $p = 0.5$ line. The phase diagram for the XY model limit, namely odd $q \to \infty$, is also shown in Fig. 2, calculated here with $q = 361$ clock states. In this limit, the distinction between odd and even q disappears. This suggests that the zero-temperature spin-glass phase [60] found for even $q \to \infty$ [21] also occurs for odd $q \to \infty$.

IV. ALGEBRAICALLY ORDERED PHASES, FINITE-TEMPERATURE RENORMALIZATION-GROUP SINKS, AND GROUND-STATE ENTROPY

Spins in odd q-state clock models cannot be exactly antialigned with each other, i.e., $\theta_i - \theta_j = 2\pi q_{ij}/q < \pi$, where q_{ij} is an integer between 0 and $(q-1)/2$ inclusive. Furthermore, for a given spin, its interacting neighbor has two states that give the maximally misaligned pair configuration with $\theta_i - \theta_j = \pi(q-1)/q < \pi$. Thus, for antiferromagnetic interaction, this local degeneracy is of crucial distinctive importance, injecting ground-state entropy into the system, driving the sink of a would-be ordered phase to nonzero temperature, and thereby causing algebraic order, as generally explained in Refs. [3,4].

All points in the antiferromagnetic phases in the phase diagrams in Figs. 2 and 3 flow under renormalization-group to $p = 1$ (just as all points in the one ferromagnetic phase flow to $p = 0$). The most extant antiferromagnetic phase in Fig. 2, labeled AF_1(alg), occurring for all odd $q \geqslant 5$ values, is an algebraically ordered phase. All points in this phase flow to a completely stable fixed point (a phase sink [61]) that is also a critical point since it occurs at finite temperature [3,4]. Of the pair-interaction Boltzmann weights $e^{V(\theta_i - \theta_j)}$, with $\theta_i - \theta_j = \pi(q - 1 - 2n)/q$, where $n = 0$ is the most misaligned pair state, $n = 1$ is the next-most misaligned state, etc., until $n = (q-1)/2$ is the completely aligned pair state, only two are nonzero at this sink: The most misaligned pair state, $n = 0$, is dominant with $e^{V(\pi(q-1)/q)} = 1$ and the next-most misaligned pair state, $n = 1$, is also present but less dominant with $e^{V(\pi(q-3)/q)} = 1/3$. The other, less misaligned pair states, with $n \geqslant 2$, and the aligned pair state have zero Boltzmann weight at this sink. That these sink fixed-point Boltzmann weights are applicable for all odd q is consistent with the fact that the $q - 5$ less-misaligned pair states and one aligned pair state have negligible Boltzmann weights at the sink fixed point, so that the numerosity of q does not matter. The finite difference between the energies for $\theta_i - \theta_j = \pi(q-1)/q$ and $\theta_i - \theta_j = \pi(q-3)/q$ establishes this sink as a finite-temperature attractive critical fixed point. It can be shown that, in the basin of attraction of a finite-temperature fixed point, the order parameter is strictly zero, the correlation length is infinite, and the correlations vanish algebraically with distance [3,4,11,62].

The evolution of the quenched probability distribution, under successive renormalization-group transformations, towards such a critical sink is shown in Fig. 4. The case of $q = 9$, starting with the initial condition temperature $1/J = 4$ and antiferromagnetic bond concentration $p = 0.8$ is shown in the figure. For $q = 9$, the generalized interaction potential unavoidably generated by the renormalization-group transformation is determined by four interaction constants (see Table I). The renormalization-group transformation gives the evolution, under scale change, of the correlated quenched probability distribution $P(V_0, V_1, V_2, V_3, V_4)$. Shown in Fig. 4 are the projections $P_0(V_0) = \int dV_1 dV_2 dV_3 dV_4 P(V_0, V_1, V_2, V_3, V_4)$ and similarly for $P_1(V_1), P_2(V_2), P_3(V_3)$, and $P_4(V_4)$. Each row corresponds to another renormalization-group step k, as marked on the figure. It is seen that in four renormalization-group transformations, the renormalized system essentially reaches the critical phase sink described above: The most misaligned pair state is dominant with Boltzmann weight $e^{V(8\pi/9)} = 1$ and the next-most misaligned pair state is also present but less dominant with $e^{V(6\pi/9)} = 1/3$. The other two less misaligned pair states and the aligned pair state have zero Boltzmann weight at the sink.

The less extant antiferromagnetic phases occur for specific q values, at lower temperatures, and are disconnected from the most extant antiferromagnetic phase AF_1(alg). In AF_2(alg), the two sink Boltzmann weights have exchanged roles: the next-most misaligned pair state, $n = 1$, is dominant with $e^{V(\pi(q-3)/q)} = 1$ and the most misaligned pair state, $n = 0$, is also present but less dominant with $e^{V(\pi(q-1)/q)} = 1/3$. In

TABLE I. Antiferromagnetic phase-transition critical fixed-point potentials $V(\pi(q-1-2n)/q)$, critical exponents y_T, and corresponding relevant eigenvectors of different odd q-state clock models. Thus, each column progresses, from left to right, from the most misaligned pair state $n=0$ to the aligned pair state $n=(q-1)/2$. For each q, the relevant eigenvector is the (only) relevant eigenvector of the $[(q-1)/2]\times[(q-1)/2]$ recursion matrix between the independent $V(\theta_{ij})$. Although the fixed points and relevant eigenvectors are distinct for different q, the critical exponents quickly converge $y_T=0.8737$.

$V(\theta_{ij})$	$n=0$	$n=1$	$n=2$	$n=3$	$n=4$	$n=5$	$n=6$	y_T	relevant eigenvectors
$q=5$	0	−0.0905	−0.1502					0.869030	(1, 0.588)
$q=7$	0	−0.0538	−0.1242	−0.1569				0.873691	(1, 0.782, 0.330)
$q=9$	0	−0.0345	−0.0893	−0.1395	−0.1599			0.873709	(1, 0.866, 0.544, 0.206)
$q=11$	0	−0.0238	−0.0649	−0.1111	−0.1475	−0.1614		0.873709	(1, 0.909, 0.675, 0.387, 0.140)
$q=13$	0	−0.0173	−0.0486	−0.0873	−0.1249	−0.1523	−0.1623	0.873709	(1, 0.935, 0.759, 0.523, 0.287, 0.101)

AF_3(alg), AF_4(alg), AF_5(alg), AF_6(alg), AF_7(alg), these roles are played respectively by $n=2,0, n=1,2, n=2,1, n=1,4$, $n=4,2$. On the other hand, AF_8(cnv) is a conventionally ordered phase, with a strong-coupling sink fixed point where $n=1$ and $n=4$ are equally dominant.

It is thus seen that the stable sink fixed points that attract, under renormalization-group flows, and characterize the algebraically ordered phases have identical structure for all odd $q\geqslant 5$. A similar, but not identical, phenomenon occurs for the unstable critical fixed points that control the antiferromagnetic phase transitions. This is seen in Fig. 5 and Table I, where the ferromagnetic ($p=0$) and antiferromagnetic ($p=1$) critical temperatures $1/J_C$ are given as a function of q. The fixed-point Boltzmann weight values $e^{V(\pi(q-1-2n)/q)}$ underpinning the antiferromagnetic phase transitions, as well as the critical exponents y_T and corresponding relevant eigenvectors are given for different q in Table I. For each q, the relevant eigenvector is the (only) relevant eigenvector of the $[(q-1)/2]\times[(q-1)/2]$ recursion matrix between the independent $V(\theta_{ij})$. Although the fixed points and relevant eigenvectors are distinct for different q, the critical temperatures and critical exponents quickly converge, for high q, to $1/J_C=12.2373$ and $y_T=0.8737$. The critical temperatures and exponents thus show differences for low q. The convergence for high q of the critical temperatures at $p=0$ and $p=1$ is expected, since the q-state clock models approach the XY model for large q, with identical antiferromagnetic and ferromagnetic behavior.

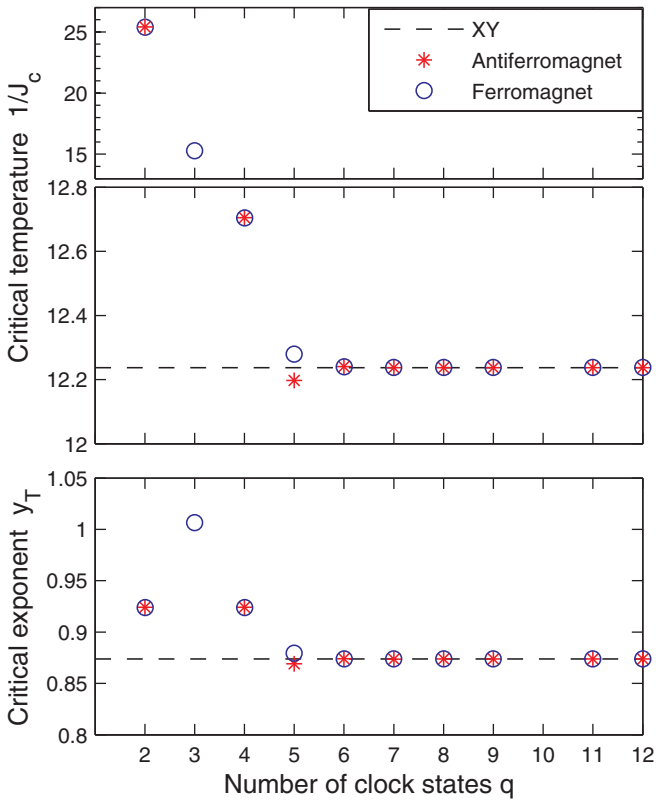

FIG. 5. (Color online) Top: Critical temperatures $1/J_C$ of the ferromagnetic (circles) and antiferromagnetic (asterisks) q-state clock models in $d=3$. Bottom: Critical exponents y_T of the ferromagnetic (circles) and antiferromagnetic (asterisks) q-state clock models in $d=3$. In both panels, the values exactly coincide for even q, due to the ferromagnetic-antiferromagnetic symmetry that is present for even q but absent for odd q.

V. CONCLUSION

We have calculated, from renormalization-group theory, the phase diagrams of arbitrary odd q-state clock spin-glass models in $d=3$. These models have asymmetric phase diagrams, as is also the case for quantum Heisenberg spin-glass models [5]. For all odd $q\geqslant 5$, algebraically ordered antiferromagnetic phases occur. One such phase is dominant and occurs for all $q\geqslant 5$. Other such phases occupy small low-temperature portions of the phase diagrams and occur for $5\leqslant q\leqslant 15$. All algebraically ordered phases have the same structure, determined by an attractive finite-temperature sink fixed point where a dominant and a subdominant pair states are the nonzero Boltzmann weights. The phase transition critical exponents, on the other hand, vary with q only at low q.

A rich and distinctive phase transition structure is thus seen for odd q-state spin-glass models on a $d=3$ dimensional hierarchical lattice.

ACKNOWLEDGMENTS

Support by the Alexander von Humboldt Foundation, the Scientific and Technological Research Council of Turkey (TÜBITAK), and the Academy of Sciences of Turkey (TÜBA) is gratefully acknowledged.

[1] H. Nishimori, *Statistical Physics of Spin Glasses and Information Processing* (Oxford University Press, Oxford, 2001).
[2] G. Toulouse, Commun. Phys. **2**, 115 (1977).
[3] A. N. Berker and L. P. Kadanoff, J. Phys. A **13**, L259 (1980).
[4] A. N. Berker and L. P. Kadanoff, J. Phys. A **13**, 3786 (1980).
[5] C. N. Kaplan and A. N. Berker, Phys. Rev. Lett. **100**, 027204 (2008); see also P. C. Menezes and A. Theumann, Phys. Rev. B **78**, 054444 (2008).
[6] A. A. Migdal, Zh. Eksp. Teor. Fiz. **69**, 1457 (1975) [Sov. Phys. JETP **42**, 743 (1976)].
[7] L. P. Kadanoff, Ann. Phys. (NY) **100**, 359 (1976).
[8] A. N. Berker and S. Ostlund, J. Phys. C **12**, 4961 (1979).
[9] R. B. Griffiths and M. Kaufman, Phys. Rev. B **26**, 5022R (1982).
[10] M. Kaufman and R. B. Griffiths, Phys. Rev. B **30**, 244 (1984).
[11] S. R. McKay and A. N. Berker, Phys. Rev. B **29**, 1315 (1984).
[12] M. Hinczewski and A. N. Berker, Phys. Rev. E **73**, 066126 (2006).
[13] M. J. P. Gingras and E. S. Sørensen, Phys. Rev. B. **46**, 3441 (1992).
[14] G. Migliorini and A. N. Berker, Phys. Rev. B. **57**, 426 (1998).
[15] M. J. P. Gingras and E. S. Sørensen, Phys. Rev. B. **57**, 10264 (1998).
[16] M. Hinczewski and A. N. Berker, Phys. Rev. B **72**, 144402 (2005).
[17] C. Güven, A. N. Berker, M. Hinczewski, and H. Nishimori, Phys. Rev. E **77**, 061110 (2008).
[18] M. Ohzeki, H. Nishimori, and A. N. Berker, Phys. Rev. E **77**, 061116 (2008).
[19] V. O. Özçelik and A. N. Berker, Phys. Rev. E **78**, 031104 (2008).
[20] G. Gülpınar and A. N. Berker, Phys. Rev. E **79**, 021110 (2009).
[21] E. Ilker and A. N. Berker, Phys. Rev. E **87**, 032124 (2013).
[22] E. Ilker and A. N. Berker, Phys. Rev. E **89**, 042139 (2014).
[23] M. Kaufman and H. T. Diep, Phys. Rev. E **84**, 051106 (2011).
[24] J. Barre, J. Stat. Phys. **146**, 359 (2012).
[25] C. Monthus and T. Garel, J. Stat. Mech. (2012) P05002.
[26] Z. Zhang, Y. Sheng, Z. Hu, and G. Chen, Chaos **22**, 043129 (2012).
[27] S.-C. Chang and R. Shrock, Phys. Lett. A **377**, 671 (2013).
[28] Y.-L. Xu, L.-S. Wang, and X.-M. Kong, Phys. Rev. A **87**, 012312 (2013).
[29] R. F. S. Andrade and H. J. Herrmann, Phys. Rev. E **87**, 042113 (2013).
[30] R. F. S. Andrade and H. J. Herrmann, Phys. Rev. E **88**, 042122 (2013).
[31] C. Monthus and T. Garel, J. Stat. Mech. (2013) P06007.
[32] O. Melchert and A. K. Hartmann, Eur. Phys. J. B **86**, 323 (2013).
[33] J.-Y. Fortin, J. Phys. Cond. Mat. **25**, 296004 (2013).
[34] Y. H. Wu, X. Li, Z. Z. Zhang, and Z. H. Rong, Chaos Solitons Fractals **56**, 91 (2013).
[35] P. N. Timonin, Low Temp. Phys. **40**, 36 (2014).
[36] B. Derrida and G. Giacomin, J. Stat. Phys. **154**, 286 (2014).
[37] M. F. Thorpe and R. B. Stinchcombe, Philos. Trans. R. Soc. A **372**, 20120038 (2014).
[38] C. Monthus and T. Garel, Phys. Rev. B **89**, 184408 (2014).
[39] T. Nogawa and T. Hasegawa, Phys. Rev. E **89**, 042803 (2014).
[40] M. L. Lyra, F. A. B. F. de Moura, I. N. de Oliveira, and M. Serva, Phys. Rev. E **89**, 052133 (2014).
[41] Y.-L. Xu, X. Zhang, Z.-Q. Liu, K. Xiang-Mu, and R. Ting-Qi, Eur. Phys. J. B **87**, 132 (2014).
[42] Y. Hirose, A. Oguchi, and Y. Fukumoto, J. Phys. Soc. Japan **83**, 074716 (2014).
[43] D. Andelman and A. N. Berker, Phys. Rev. B **29**, 2630 (1984).
[44] Y. Qin and Z. R. Yang, Phys. Rev. B **43**, 8576 (1991).
[45] H. Saleur, Nucl. Phys. B **360**, 219 (1991).
[46] J. A. Redinz, A. C. N. deMagalhaes, and E. M. F. Curado, Phys. Rev. B **49**, 6689 (1994).
[47] J. A. Redinz and A. C. N. Demagalhaes, Physica A **246**, 27 (1997).
[48] J. L. Jacobsen, J. Salas, and A. D. Sokal, J. Stat. Phys. **119**, 1153 (2005).
[49] J. L. Jacobsen and H. Saleur, Nucl. Phys. B **743**, 207 (2006).
[50] Y. Ikhlef, Mod. Phys. Lett. B **25**, 291 (2011).
[51] J. L. Jacobsen and C. R. Scullard, J. Phys. A **45**, 494003 (2012).
[52] J. L. Jacobsen and J. Salas, Nucl. Phys. B **875**, 678 (2013).
[53] J. M. Kosterlitz and D. J. Thouless, J. Phys. C **6**, 1181 (1973).
[54] J. V. José, L. P. Kadanoff, S. Kirkpatrick, and D. R. Nelson, Phys. Rev. B **16**, 1217 (1977).
[55] A. N. Berker and D. R. Nelson, Phys. Rev. B **19**, 2488 (1979).
[56] J. O. Indekeu and A. N. Berker, Physica A **140**, 368 (1986).
[57] R. R. Netz and A. N. Berker, Phys. Rev. Lett. **68**, 333 (1992).
[58] M. G. Mazza and M. Schoen, Int. J. Mol. Sci. **12**, 5352 (2011).
[59] S. Chen, H.-B. Luo, H.-L. Xie, and H.-L. Zhang, J. Polymer Sci. A **51**, 924 (2013).
[60] G. Grinstein, A. N. Berker, J. Chalupa, and M. Wortis, Phys. Rev. Lett. **36**, 1508 (1976).
[61] A. N. Berker and M. Wortis, Phys. Rev. B **14**, 4946 (1976).
[62] M. E. Fisher and A. N. Berker, Phys. Rev. B **26**, 2507 (1982).